JOURNAL OF CATALYSIS 55, 373–383 (1978)

Oxidation of Butene to Maleic Anhydride

II. Effect of Physical Transport on Reactor Performance

R. L. VARMA AND D. N. SARAF[1]

Department of Chemical Engineering, Indian Institute of Technology, Kanpur, Kanpur-208016, India

Received December 13, 1977; revised July 27, 1978

Effects of heat and mass transfer resistances on yield and selectivity were estimated for an exothermic multiple reaction, namely, butene oxidation to maleic anhydride over a vanadyl phosphate catalyst. The mathematical model of the catalyst pellet accounted for intraparticle concentration gradients and interphase concentration and temperature gradients. The catalyst particle was found to be essentially isothermal. Product distribution and axial temperature profiles were measured under varying operating conditions in a fixed bed reactor. A comparison between the experimental data and results predicted by the heterogeneous model of the reactor showed a fairly good agreement. Minor discrepancies observed could be attributed to the sensitivity of predicted results on certain parameters.

INTRODUCTION

It is well known that the observed rates of chemical reactions can be significantly affected by physical transport properties which include intraparticle and interphase heat and mass transfer resistances. The temperature and concentration gradients can influence the conversion, product distribution, and stability of the reactor. The effect of diffusional limitations on reactor performance has been extensively studied for the past few years (*1*, *2*). Most of the studies, however, are confined to single reactions. Relatively few workers (*3–7*) have dealt with the selectivity problems of multiple reaction systems in presence of physical effects, and comparative studies between the reactor model predictions and experimental measurements under these conditions are rather meager.

This paper deals with the experimental and theoretical evaluation of the effects of transport processes on the performance of a fixed bed reactor wherein an exothermic multiple reaction is taking place. Selective oxidation of butene to maleic anhydride over a V-P-O catalyst has been chosen as the test reaction. This reaction system was chosen owing to the recent interest in the C_4 process for making maleic anhydride (*8*). The kinetic model for this reaction was proposed in Part I of this series. The derived rate expressions based on pseudo-first-order kinetics valid under conditions of low hydrocarbon concentration were used for computational purposes. Thus, for the reaction scheme III (Part I)

$$R_1 = (k_1 + k_2)p_1 \tag{1}$$

$$R_2 = k_1p_1 - (k_3 + k_4)p_2 \tag{2}$$

$$R_3 = k_3p_2 \tag{3}$$

[1] To whom all correspondence should be addressed.

0021-9517/78/0553-0373$02.00/0

NOMENCLATURE

A_i	the ith component in a chemical reaction network
A_j^0	pre-exponential factor in Arrhenius rate expression for reaction step j
a_m	surface area per unit mass of catalyst pellet, $3/r_p\rho_p$, cm²/g
Bi_p	particle Biot number, $h_{fp}d_p/k_{ep}$
C_f	specific heat of fluid, cal/g °C
D_{ep}	effective diffusivity in porous catalyst, cm²/sec
D'_{ep}	D_{ep}/R_gT, g moles/cm atm sec
d_t	diameter of reactor tube, cm
d_p	diameter of particle, cm
E_j	activation energy for reaction step j, cal/g mole
F_t	total molar flow rate, g moles/sec
G	specific mass flow rate, g/cm² sec
h_{fp}	fluid–particle heat transfer coefficient, cal/cm² sec °C
$-\Delta H_1$, $-\Delta H_2$, $-\Delta H_3$, $-\Delta H_4$	heats of reaction for reaction steps 1, 2, 3, and 4, respectively
J_h	j-factor for heat transfer, $h_{fp}(Pr)^{\frac{2}{3}}/C_fG$
J_d	j-factor for mass transfer, $k_{fp}PM_m(Sc)^{\frac{2}{3}}/G$
k_j	reaction rate constant for reaction step j, g moles/g cat atm sec
k_f	thermal conductivity of fluid, cal/sec cm °C
k_{fp}	fluid-particle mass transfer coefficient, g moles/cm² sec atm
k_{ep}	effective thermal conductivity of catalyst particle, cal/cm sec °C
M_m	molecular weight of feed gas
m_p	mass of catalyst pellet, (4/3) $\pi r_p^3\rho_p$, g
P	total pressure, atm
Pr	Prandtl number, $C_f\mu/k_f$
p_i	partial pressure of component A_i, atm
p_{o1}	partial pressure of component A_1 in feed, atm
R_i	reaction rate of species A_i, g moles/g cat sec
$\bar{R}_i$	overall reaction rate of species A_i, g moles/g cat sec
R_g	gas constant, cal/g mole or cm³ atm/g mole °C
Re_p	Reynolds number based on particle diameter
r_p	radius of catalyst particle, cm
S_g	surface area per unit mass of catalyst, cm²/g
Sc	Schmidt number
S_{p_i}	point selectivity of a component, Eqs. (20) and (21)
S_{ov_i}	overall selectivity of a component, Y_i/x
Sh	modified Sherwood number, $r_pk_{fp}/3D'_{ep}$
s	radial particle coordinate, cm
T	temperature, K
T_c	coolant temperature or inlet fluid temperature, K
ΔT_{max}	maximum temperature rise within the pellet, $T_{max} - T_s$, °C
U	overall heat transfer coefficient, cal/cm² sec K
V_g	pore volume per unit mass of catalyst, cm³/g
W	weight of catalyst, g
X	conversion of component A_1
Y_i	yield of component i moles of A_i in product/moles of reactant A_1 in feed

Greek Symbols

ϵ_b	void fraction of the bed
ϵ_p	void fraction of the particle
η	effectiveness factor
μ	fluid viscosity, g/cm sec
π	3.14159
ρ_f	density of fluid, g/cm³
ρ_p	density of catalyst particle, g/cm³
σ	tortuosity factor
τ_t	time factor based on total feed rate, W/F_t, g cat sec/g mole

NOMENCLATURE (*Continued*)

Subscripts

s	surface of pellet	i	designating which component
b	bulk fluid conditions	j	designating which reaction

EXPERIMENTAL

Selective oxidation of butene to maleic anhydride was studied in an integral reactor immersed in a molten salt bath. Details of the apparatus and experimental methods were same as described in Part I and elsewhere (*9*). The temperature of the catalyst bed was measured at several locations along the axis of the reactor. As already reported in Part I, isothermal conditions were maintained by diluting the catalyst with an inert material. Non-isothermal runs were carried out without diluting the catalyst and maintaining the temperature of the inlet stream equal to that of the salt bath. The ranges of operating variables were as follows: partial pressure of butene in feed, 0.0078 to 0.01 atm; inlet temperature, 350 to 400°C; time factor, τ_t, 1.43×10^3 to 48.5×10^3 g of catalyst sec/g mole; weight of catalyst, 5.79 to 99.0 g.

The catalyst employed was V-P-O (P/V atomic ratio = 1.6) supported on silica gel of −8- to +10-mesh size. Surface area of the catalyst was determined by the BET method from nitrogen adsorption isotherms. Pore volume and pore size distribution were measured by a mercury porosimeter, Carlo-Erba Model-70, for the 2000 atmospheric range. The physical properties of the catalyst are given in Table 1.

TABLE 1

Physical Properties of V-P-O Catalyst

ρ_p(g/cm³)	V_g(cm³/g)	ϵ_p	s_g(m²/g)
0.99	0.3952	0.391	85

TABLE 2

Data for Pellet and Reactor Models

r_p	= 0.1 cm
ρ_p	= 0.99 g/cm³
Pr	= 0.69
Sc	= 1.5
C_f	= 0.25 cal/g °C
M_m	= 29.2
μ	= 0.31×10^{-3} g/cm sec
ρ_f	= 0.524×10^{-3} g/cm³
F_t	= 4.5×10^{-3} g moles/sec
d_t	= 2.5 cm
ϵ_b	= 0.42
U	= 2.3×10^{-3} cal/cm² sec
$-\Delta H_1$	= 35 kcal/g mole
$-\Delta H_2$	= 640 kcal/g mole
$-\Delta H_3$	= 270 kcal/g mole

MATHEMATICAL MODEL OF THE CATALYST PELLET

The evaluation of transport resistances requires a model for the catalyst pellet accounting for these effects. Since the particle equations must be solved along with the external field equations in order to study the reactor performance, the consideration of a fully distributed pellet model involves excessive computational efforts, which may be prohibitive for routine design purposes. Considerable reduction in computational time can be achieved by making some reasonable approximations. An approximate model for the catalyst pellet which has been widely used with justification is the "lumped thermal resistance model" (*10–12*). This approach assumes that the entire heat transfer resistance lies in the external film, so that the pellet is essentially iso-

thermal. The validity and usefulness of this model has been discussed extensively (*4, 12, 13*). Based on this assumption, the steady-state mathematical description of heat and mass transport effects is given as

$$h_{fp}a_m(T_s - T_b) = (-\Delta H_2)\bar{R}_1 - (-\Delta H_4)\bar{R}_2 + [(-\Delta H_3) - (-\Delta H_4)]\bar{R}_3 \quad (4)$$

$$\frac{1}{s^2}\frac{D_{ep}}{R_gT}\frac{d}{ds}\left(s^2\frac{dp_1}{ds}\right) - \rho_p R_1 = 0 \quad (5)$$

$$\frac{1}{s^2}\frac{D_{ep}}{R_gT}\frac{d}{ds}\left(s^2\frac{dp_2}{ds}\right) + \rho_p R_2 = 0 \quad (6)$$

$$\frac{1}{s^2}\frac{D_{ep}}{R_gT}\frac{d}{ds}\left(s^2\frac{dp_3}{ds}\right) + \rho_p R_3 = 0, \quad (7)$$

with boundary conditions

$$dp_1/ds = dp_2/ds = dp_3/ds = 0 \quad \text{at} \quad s = 0 \quad (8)$$

$$\left.\begin{aligned}\frac{D_{ep}}{R_gT}\frac{dp_1}{ds} &= k_{fp}(p_{b1} - p_1)\\ \frac{D_{ep}}{R_gT}\frac{dp_2}{ds} &= k_{fp}(p_{b2} - p_2)\\ \frac{D_{ep}}{R_gT}\frac{dp_3}{ds} &= k_{fp}(p_{b3} - p_3)\end{aligned}\right\} \text{at } s = r_p. \quad (9)$$

The overall reaction rates expressed in terms of mass fluxes at the pellet surface are

$$\bar{R}_1 = \frac{1}{m_p}4\pi r_p^2\frac{D_{ep}}{R_gT}\left(\frac{dp_1}{ds}\right)_{s=r_p} = \frac{3}{r_p\rho_p}\frac{D_{ep}}{R_gT}\left(\frac{dp_1}{ds}\right)_{s=r_p} \quad (10)$$

$$\bar{R}_2 = -\frac{3}{r_p\rho_p}\frac{D_{ep}}{R_gT}\left(\frac{dp_2}{ds}\right)_{s=r_p} \quad (11)$$

$$\bar{R}_3 = -\frac{3}{r_p\rho_p}\frac{D_{ep}}{R_gT}\left(\frac{dp_3}{ds}\right)_{s=r_p}. \quad (12)$$

The validity of the isothermal pellet model can be checked. For the reaction scheme under consideration, maximum temperature rise within the pellet may be expressed as

$$\Delta T_{max} = \frac{D'_{ep}}{k_{ep}}(-\Delta H_2)p_{s1} + (-\Delta H_4)p_{s2} + [(-\Delta H_4) - (-\Delta H_3)]p_{s3}, \quad (13)$$

where $D'_{ep} = D_{ep}/R_gT$.

The above expression follows from an analysis similar to that of Prater (*14*). Typical values of parameters D'_{ep} and k_{ep}, measured for commonly used catalysts are available in the literature (*1*). Thus taking $D'_{ep} = 0.8 \times 10^{-6}$ g moles/cm atm sec, $k_{ep} = 7.5 \times 10^{-3}$ cal/cm sec K, and partial pressure of each component = 0.003 atm, we find

$$\Delta T_{max} = 0.505°C.$$

This estimate shows that the pellet is essentially isothermal.

Solution of Single-Particle Equations

The solution of Eqs. (5) to (7) with the associated boundary conditions gives

$$p_1 = \frac{r_p}{s}\frac{p_{b1}}{m_1}\frac{\sinh(3s/r_p[\alpha_{12}]^{\frac{1}{2}})}{\sinh(3[\alpha_{12}]^{\frac{1}{2}})} \quad (14)$$

$$p_2 = \frac{r_p}{s}\frac{p_{b1}}{m_1}\left[\frac{p_{b2}}{p_{b1}} + \frac{\alpha_1}{\alpha_{1234}}\right] \times \frac{\sinh(3s/r_p[\alpha_{34}]^{\frac{1}{2}})}{\sinh(3[\alpha_{34}]^{\frac{1}{2}})} - \frac{\alpha_1}{\alpha_{1234}}p_1 \quad (15)$$

$$p_3 = p_{b3} + \frac{\alpha_1\alpha_3}{\alpha_{12}\alpha_{34}}(p_{b1} - p_1) + \frac{\alpha_3}{\alpha_{34}}(p_{b2} - p_2), \quad (16)$$

where

$$\alpha_{12} = \alpha_1 + \alpha_2$$

$$\alpha_{34} = \alpha_3 + \alpha_4$$

$$\alpha_{1234} = \alpha_{12} - \alpha_{34}$$

$$\alpha_j = \frac{r_p^2}{9}\frac{\rho_p}{D'_{ep}} k_j \quad (j = 1, 2, 3, 4)$$

$$k_j = A_j^0 \exp(-E_j/R_g T_s)$$

$$m_1 = 1 + \frac{1}{\mathrm{Sh}}\left[(\alpha_{12})^{\frac{1}{2}} \coth\left(3\{\alpha_{12}\}^{\frac{1}{2}}\right) - \tfrac{1}{3}\right]$$

$$m_2 = 1 + \frac{1}{\mathrm{Sh}}\left[(\alpha_{34})^{\frac{1}{2}} \coth\left(3\{\alpha_{34}\}^{\frac{1}{2}}\right) - \tfrac{1}{3}\right]$$

$$\mathrm{Sh} = r_p k_{fp}/3D'_{ep}.$$

Substituting Eqs. (14) to (16) into Eqs. (10) to (12) gives expressions for overall reaction rates

$$\bar{R}_1 = \frac{9D'_{ep}}{r_p^2 \rho_p}\frac{\alpha_{12}}{m_1}\eta_1 p_{b1} \tag{17}$$

$$\bar{R}_2 = \frac{\alpha_1 \bar{R}_1}{\alpha_{1234}} - \frac{m_1}{m_2}\frac{\alpha_{34}}{\alpha_{12}}\frac{\eta_2}{\eta_1}\left[Q + \frac{\alpha_1}{\alpha_{1234}}\right]\bar{R}_1 \tag{18}$$

$$\bar{R}_3 = \frac{\alpha_1 \alpha_3 \bar{R}_1}{\alpha_{12}\alpha_{34}} - \frac{\alpha_3}{\alpha_{34}}\bar{R}_2, \tag{19}$$

where

$$\eta_1 = \frac{1}{\alpha_{12}}\left[(\alpha_{12})^{\frac{1}{2}} \coth\left(3\{\alpha_{12}\}^{\frac{1}{2}}\right) - \tfrac{1}{3}\right]$$

$$\eta_2 = \frac{1}{\alpha_{34}}\left[(\alpha_{34})^{\frac{1}{2}} \coth\left(3\{\alpha_{34}\}^{\frac{1}{2}}\right) - \tfrac{1}{3}\right]$$

$$Q = p_{b2}/p_{b1}$$

Substitution of overall rates of reaction given by Eqs. (17) to (19) into the heat balance equation (4) would give an algebraic expression, the right-hand side of which would be a nonlinear function of T_s. The solution of the equation is obtained, as in this work, by the method of successive substitutions. The overall rates of reaction thus evaluated are used to calculate the effectiveness factor and local selectivities. Local selectivity for component A_2, defined as the ratio of production of A_2 to the rate of depletion of A_1 is given by

$$S_{p2} = \left.\frac{(-dp_2/ds)}{(dp_1/ds)}\right|_{s=r_p} = \frac{\bar{R}_2}{\bar{R}_1}. \tag{20}$$

Similarly, the selectivity of component A_3 is

$$S_{p3} = \frac{\bar{R}_3}{\bar{R}_1} \tag{21}$$

The effectiveness factor, η_b, defined as the ratio of effective rate of disappearance of initial substance A_1 to the rate of disappearance at bulk fluid conditions is given by

$$\eta_b = \frac{\bar{R}_1}{R_{b1}} = \frac{(\alpha_1 + \alpha_2)}{(\alpha_1 + \alpha_2)_b}\frac{\eta_1}{m_1} \tag{22}$$

COMPUTATION OF CATALYST EFFECTIVENESS AND SELECTIVITY

The model of the catalyst pellet was solved to evaluate the effectiveness factor and selectivity, using the rate expressions representative of kinetics of butene oxidation to maleic anhydride. Computations were carried out for fixed values of concentration and temperature in the bulk fluid. Data for the model including fluid and solid properties are summarized in Table 2.

The confidence in calculated results lies to a great extent on reliability of values of transport parameters employed (*15*, *16*). Of the parameters estimated by correlations and models available in the literature, the prediction of effective diffusivity may not be reliable. Although various models are available for estimation of this parameter, the predictions may differ from

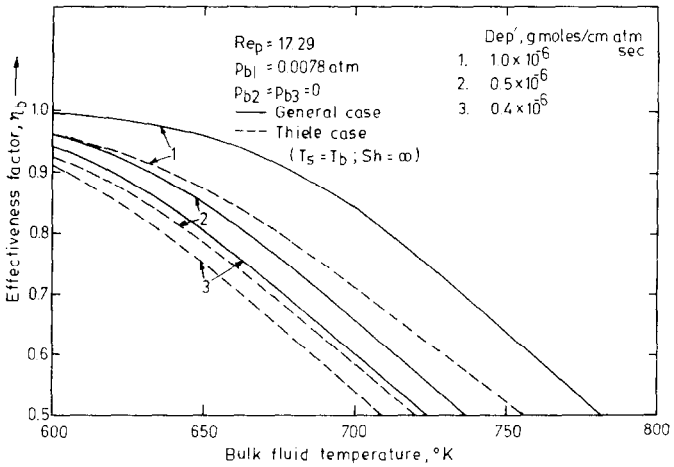

FIG. 1. Catalyst effectiveness factor vs bulk temperature for selected values of effective diffusivity.

the true value by as much as 100% (*2*). In the absence of experimental value, computations have been carried out over a range of values of practical interest. The *j*-factors for heat and mass transport at the solid surface were calculated using correlations from DeAcetis and Thodos (*17*) and Petrovic and Thodos (*18*) given by Eqs. (23) and (24), respectively

$$J_h = \frac{h_{fp}(\mathrm{Pr})^{\frac{2}{3}}}{GC_f} = \frac{1.10}{(R_{ep})^{0.41} - 0.15} \quad (23)$$

$$J_d = \frac{k_{fp}PM_m(\mathrm{Sc})^{\frac{2}{3}}}{G} = \frac{0.357}{\epsilon_b(R_{ep})^{0.359}} \quad (24)$$

RESULTS

Figure 1 shows effectiveness factor as a function of bulk fluid temperature for selected values of effective diffusivity. The effectiveness factors predicted by the general model at low temperatures (<650 K) approach unity, thus indicating kinetic control. At higher temperatures, however, physical effects seem to play a significant role. Effectiveness factors for the Thiele case (neglecting film transport) are lower than unity, indicating the existence of intraparticle concentration gradients. The effect of internal transport on overall rate of butene depletion is masked due to heat transport effects across the film. While the reaction rate is reduced due to an intraparticle concentration gradient, a temperature gradient across the film has the opposite influence. The results indicate the precision required in the estimation of effective diffusivity. The effects of internal transport on overall rate are found to be

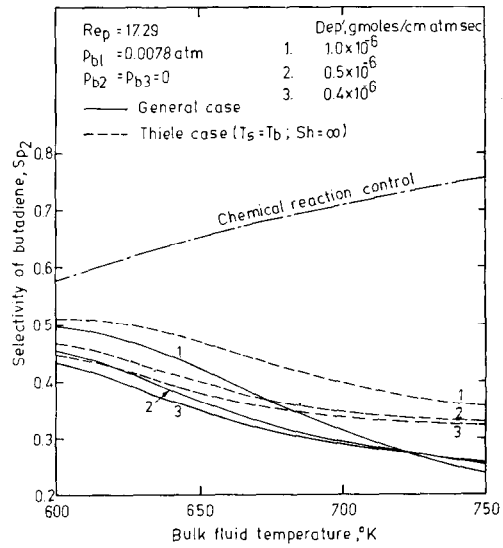

FIG. 2. Selectivity of butadiene vs bulk temperature for selected values of effective diffusivity.

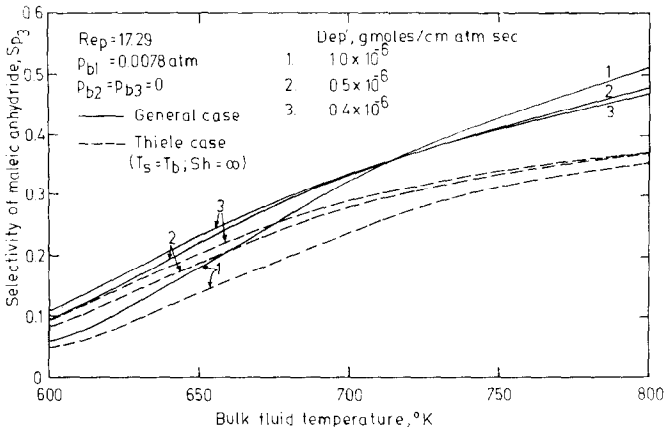

FIG. 3. Selectivity of maleic anhydride vs bulk temperature for selected values of effective diffusivity.

significant for lower values of this parameter.

Transport resistance appreciably reduce the instantaneous selectivity of the intermediate product, butadiene, and improve the selectivity of the end product, maleic anhydride. This is shown in Figs. 2 and 3.

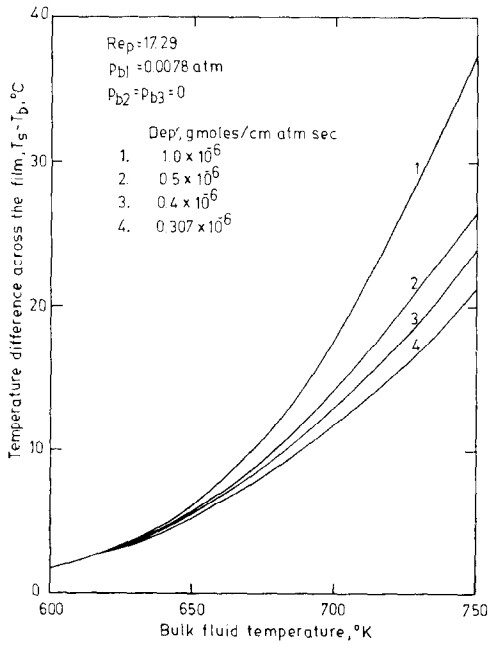

FIG. 4. Rise in pellet temperature across the film vs bulk temperature for selected values of effective diffusivity.

The temperature gradient across the film has been plotted against bulk fluid temperature for various values of D'_{ep} in Fig. 4. At lower bulk fluid temperature, the results reveal an insignificant rise in temperature with little dependence on effective diffusivity. As the bulk fluid temperature increases, $T_s - T_b$ increases rapidly, being higher for higher values of D'_{ep}. The physical reality that the film heat transfer resistance dominates the intraparticle resistance can be shown using a criterion given by Mears (*19*). The estimation of particle Biot number, a measure of the ratio of intraparticle to fluid particle heat transfer gives

$$Bi_p = h_{fp}d_p/k_{ep} = 0.94$$

which is far below 10.

Simulation of the Packed-Bed Catalytic Reactor—Comparison with the Experimental Data

The influence of transport effects on the performance of the packed-bed reactor was examined. The basic conservation equations for the fluid phase can be combined with the pellet model to give the complete description of the system (*20*). The one-dimensional model for the fluid field was used; this approximation has

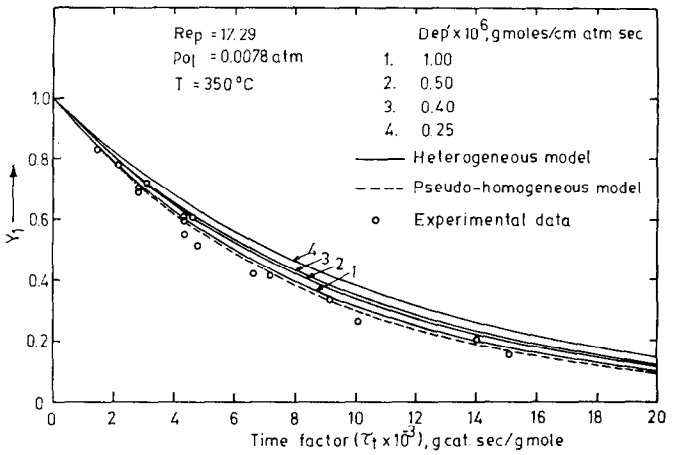

FIG. 5. Conversion of butene vs time factor; comparison between homogeneous and heterogeneous models at 350°C.

been frequently found valid particularly when the tube diameter is not too large (*3, 21*). The predicted results from the heterogeneous model and a simple pseudo-homogeneous model (neglecting pellet effects) were compared with the experimental observations.

Isothermal Operation

In Figs. 5 and 6, are compared the conversions of butene predicted by the two models at 350 and 390°C. The agreement with the experimental data is excellent except for unusually low values of effective diffusivity. Similar conclusions may be drawn for the yield curves of maleic anhydride (Figs. 7 and 8). For low values of effective diffusivity, internal transport becomes significant, and therefore a lower conversion of butene is obtained. This leads to lower yield of maleic anhydride. Figure 9 shows the effect of internal diffusion on overall selectivity of maleic anhydride. Internal transport causes slight increase in the selectivity at lower

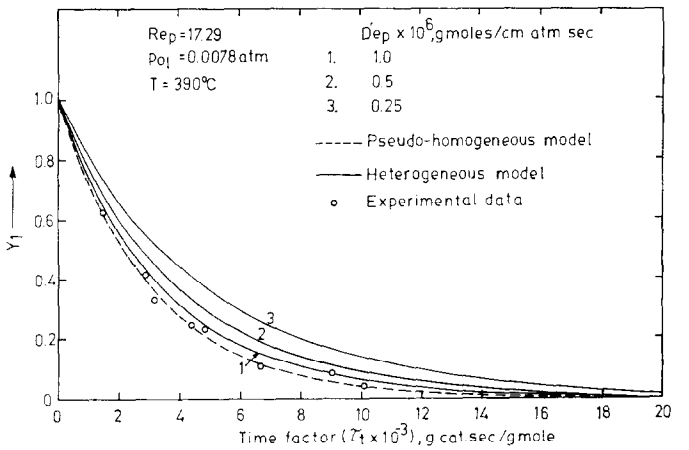

FIG. 6. Conversion of butene vs time factor; comparison between homogeneous and heterogeneous models at 390°C.

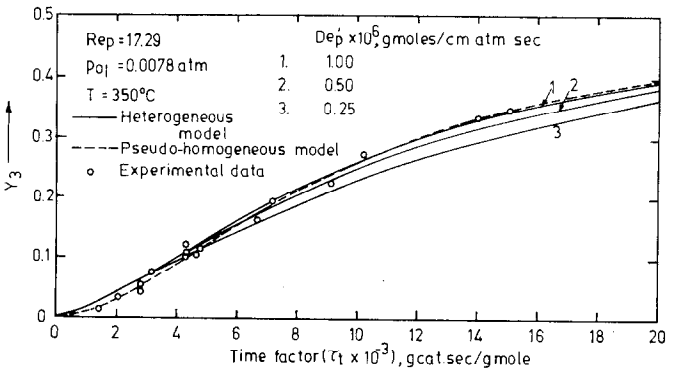

FIG. 7. Yield of maleic anhydride vs time factor; comparison between homogeneous and hetrogeneous models at 350°C.

conversion, but has little influence at high conversion.

Above comparisons were made for the feed containing 0.78 mole% butene in air at 350 and 390°C. Comparing the results obtained at other operating conditions led to similar conclusions. The agreement between the experimental data and the predictions in the reactor model incorporating pellet effects for $D'_{ep} = 10^{-6}$ g moles/cm atm sec, which is a reasonable value for the catalyst employed, was rather remarkable.

Nonisothermal Operation

Calculations based on a pseudohomogeneous reactor model predicted a runaway region. All subsequent computations were performed with the heterogeneous model (accounting for physical transport). In Fig. 10 is presented a typical comparison between the experimental and predicted axial temperature profiles for selected values of effective diffusivity. It is seen that the predicted temperature is highly sensitive to chosen value of D'_{ep} and increases more sharply for higher values of D'_{ep} at which the calculated temperature of the hot spot is much higher than the observed temperature. The predicted yield of maleic anhydride is also slightly higher than the experimental values as shown in Table 3. It is to be emphasized that the

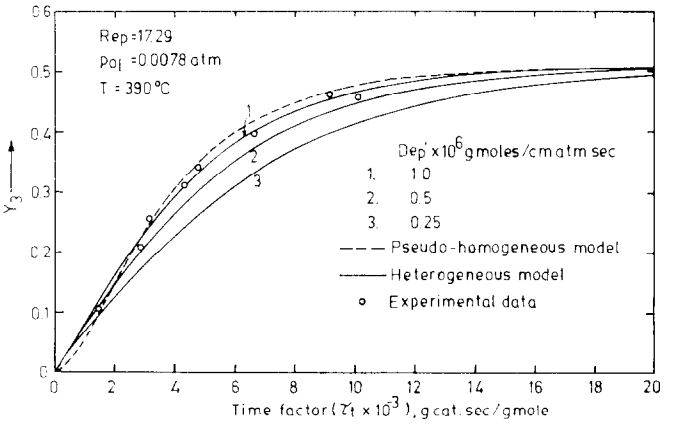

FIG. 8. Yield of maleic anhydride vs time factor; comparison between homogeneous and hetrogeneous models at 390°C.

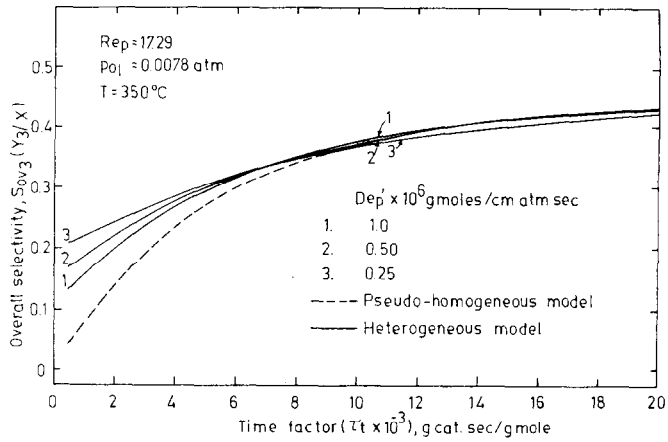

FIG. 9. Overall selectivity of maleic anhydride vs time factor; comparison between homogeneous and heterogeneous models at 350°C.

kinetic model used for computation was derived based on isothermal operation at 350 to 390°C, and therefore the simulation results for nonisothermal operation at higher temperatures may represent a gross extrapolation of the model. In view of the high temperatures and the sensitive region encountered in nonisothermal runs, the agreement between the observed and predicted results seems to be acceptable. These results demonstrate a test of the kinetic model under severe operating conditions.

Parametric sensitivity tests of the reactor model serve to identify the parameters which must be estimated more accurately. The results have clearly shown that there is a need for experimental measurement of effective diffusivity. In addition, the measurement of fluid–solid heat and mass transfer coefficients under reaction conditions is desirable. In cases

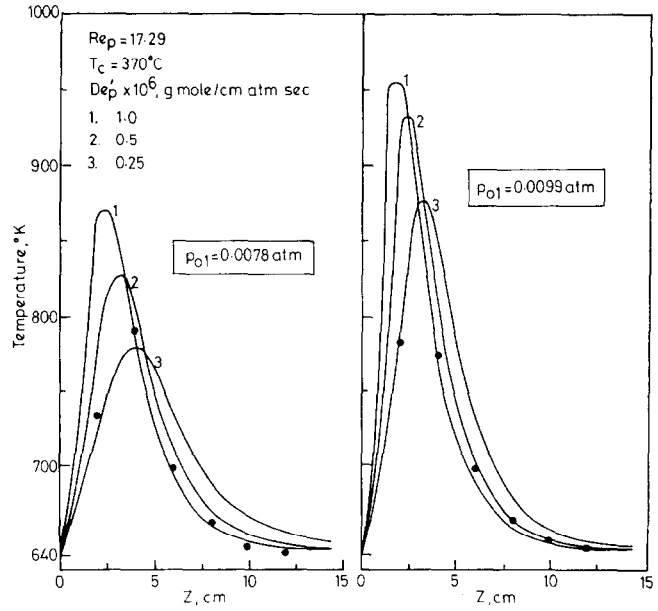

FIG. 10. Calculated and measured axial temperature profiles.

TABLE 3

Experimental and Predicted Yield of Maleic Anhydride

Inlet temperature, T_c (K)	p_{o1} (atm)	$\tau_t \times 10^{-3}$ g of catalyst sec/g·mole	Yield of maleic anhydride, Y_3			
			Experimental	Calculated		
				$D'_{ep} \times 10^6$ (g·moles/cm atm sec)		
				1.0	0.25	0.2
623	0.0078	15.1	0.349	0.587	0.499	0.478
623	0.0099	24.1	0.406	0.639	0.575	0.554
643	0.0078	24.1	0.462	0.621	0.571	0.558
643	0.0099	17.9	0.445	0.661	0.619	0.606
663	0.0078	10.1	0.459	0.643	0.60	0.586
663	0.0099	24.1	0.491	0.677	0.646	0.635

where precise estimates of transport parameters are available, the proposed mathematical model could be used for further refinement of intrinsic kinetic parameters with the help of a minimization technique.

CONCLUSIONS

An isothermal pellet model for the system involving parallel and consecutive reactions representative of butene oxidation to maleic anhydride was developed. The effects of transport processes including intrapellet mass transfer and interphase heat and mass transfer on conversion and selectivity were estimated. It is observed that the major resistance to heat transfer lies in the external film, whereas the mass transfer effects are significant within the catalyst. The assumption of pellet isothermality is valid for all practical purposes.

The models of the packed-bed reactor predict conversion and product distribution which are in reasonable agreement with the experimental results. Parameteric sensitivity tests over this model could be used to identify the parameters which need be estimated more accurately.

REFERENCES

1. Satterfield, C. N., "Mass Transfer in Heterogeneous Catalysis." M.I.T. Press, Cambridge, Mass., 1970.
2. Smith, J. M., *J. Chem. Eng. Japan* **6**, 191 (1973).
3. Cresswell, D. L., and Paterson, W. R., *Chem. Eng. Sci.* **25**, 1405 (1970).
4. McGreavy, C., and Thornton, J. M., *Chem. Eng. Sci.* **25**, 303 (1970).
5. Carberry, J. J., *Chem. Eng. Sci.* **17**, 675 (1962).
6. Wirges, H. P., and Rahse, W., *Chem. Eng. Sci.* **30**, 647 (1975).
7. Trimm, D. L., Corrie, J., and Holton, R. D., *Chem. Eng. Sci.* **29**, 2009 (1974).
8. Ushio, S., *Chem. Eng. (New York)* **78**, 107 (1971).
9. Varma, R. L., Ph.D. thesis, Department of Chemical Engineering, Indian Institute of Technology, Kanpur, 1976.
10. Carberry, J. J., and Wendel, M. M., *AIChE J.* **9**, 129 (1963).
11. Carberry, J. J., and White, D., *Ind. Eng. Chem.* **61**, 27 (1969).
12. McGreavy, C., and Cresswell, D. L., *Canad. J. Chem. Eng.* **47**, 583 (1969).
13. Hlavacek, V., and Kubicek, M., *Chem. Eng. Sci.* **25**, 1961 (1970).
14. Prater, C. D., *Chem. Eng. Sci.* **8**, 284 (1958).
15. Froment, G. F., *Ind. Eng. Chem.* **59**, 18 (1967).
16. Priestely, A. J., and Agnew, J. B., *Ind. Eng. Chem. Process Des. Develop.* **14**, 171 (1975).
17. De Acetis, J., and Thodos, G., *Ind. Eng. Chem.* **52**, 1003 (1960).
18. Petrovic, L. J., and Thodos, G., *Ind. Eng. Chem. Fundam.* **7**, 274 (1968).
19. Mears, D. E., *Ind. Eng. Chem. Process Des. Develop.* **10**, 541 (1971).
20. Karanth, N. G., and Hughes, R., *Catal. Rev.* **9**, 169 (1974).
21. Paris, J. R., and Stevens, W. F., *Canad. J. Chem. Eng.* **48**, 100 (1970).